Cell-intrinsic Innate Immune Responses against Chikungunya Virus in a Human *Ex Vivo* Synovial Fibroblast Model

Fabian Pott[a,b,e], Richard J. P. Brown[c], Elena Neumann[d], Thomas Pietschmann[e], and Christine Goffinet[a,b,e*]

[a]Institute for Virology, Charité – Universitaetsmedizin Berlin, Berlin, Germany,

[b]Berlin Institute of Health, Berlin, Germany

[c]Division of Veterinary Medicine, Paul Ehrlich Institute, Langen, Germany

[d]Internal Medicine and Rheumatology, Justus-Liebig-University Giessen, Campus Kerckhoff, Bad Nauheim, Germany

[e]Institute of Experimental Virology, Twincore Centre for Experimental and Clinical Infection Research, Hannover, Germany

*Corresponding author:

Christine Goffinet, Institute for Virology, Charité – Universitaetsmedizin Berlin, Charitéplatz 1, 10117 Berlin, Germany, christine.goffinet@charite.de

Abstract

In recent years, newly and re-emerging arboviruses including Chikungunya virus (CHIKV), have caused growing concern due to expansion of insect vector ranges, mediated by the exponential increase in international travel and accelerating climate change. Due to the absence of specific antiviral treatment strategies and a protective vaccine, over 2 million CHIKV cases have been reported since 2005. Long-term morbidity after CHIKV infection includes debilitating chronic joint pain, which has associated health, social, individual, and economic impact. Here, we analyzed the early cell-intrinsic response to CHIKV infection in primary human synovial fibroblasts. This cell type represents a potential source of polyarthralgia induced by CHIKV infection. Synovial fibroblasts from healthy donors and osteoarthritic patients were similarly permissive to CHIKV infection. We observed a CHIKV infection-induced transcriptional profile that consisted in upregulation of several hundred interferon-stimulated genes, in addition to transcription factor-encoding genes and effector genes of proinflammatory pathways. In contrast, IL-6, which mediates chronic synovitis by stimulating neutrophil and macrophage infiltration into the joints, was barely secreted by CHIKV-infected fibroblasts. Finally, the cell-intrinsic response to interferon type I and III treatment of synovial fibroblasts differed from that of immortalized model cell lines. In synovial fibroblasts, CHIKV replication was impaired by IFN-α administered post-infection. In summary, primary human synovial fibroblasts serve as *bona-fide ex vivo* primary cell model of CHIKV infection and provide a valuable platform for studies of joint tissue-associated aspects of CHIKV immunopathogenesis.

Keywords: chikungunya virus, primary cells, fibroblasts, innate immunity, RNA-seq, transcriptomics

Introduction

Chikungunya virus (CHIKV) is an arthritogenic alphavirus of the *Togaviridae* family, which is transmitted by mosquitoes and circulates both in urban cycles between vectors and humans, and in sylvatic cycles [1,2]. Beyond the typically short acute phase associated with febrile illness and rashes, the most severe consequence of a CHIKV infection in humans is excruciating pain in multiple joints. The arthritis-like pain often manifests during the acute phase of the infection, but importantly can persist in a subgroup of patients for months to years [3,4]. The symptoms cause a severe loss of quality of life and high economic costs, which is a burden especially for low-income countries [5]. The underlying pathophysiology of the chronic symptoms remains largely unclear, but appears to associate with circulating IL-6 [6] and IL-12 [7]. Furthermore, it may involve persisting viral RNA [7,8], although this scenario has been debated [9].

Multiple studies on CHIKV in immortalized model cell lines or *in vivo* in immunodeficient mice have provided valuable information on key aspects of CHIKV tropism and replication, including host factors for entry and replication [10,11], the impact of mutations in the viral glycoproteins on cell entry [12], and cellular restrictions factors acting against CHIKV [13,14]. Additionally, studies investigating immune responses to infection have demonstrated that CHIKV nsP2 counteracts host immunity by blocking nuclear translocation of STAT1 [15,16] and inducing a host transcriptional shutdown [17,18]. However, it is unclear how relevant these and potentially additionally immunity-subverting mechanisms are in infected patients. *In vivo* studies in mice, though combining innate and adaptive immune responses, require a type I IFN-deficient background, neglecting the impact of type I IFN-mediated antiviral responses [19]. However, type I IFN induced in and acting on nonhematopoietic cells appears to be essential for the control and early clearance of CHIKV *in vivo* [20-22]. Therefore, these systems do not fully recapitulate the cellular

environment of human primary cells and tissues that are targeted by CHIKV *in vivo*. Primary human cells have been used sporadically, but only few studies properly characterized their unique properties [23-25]. Here, we perform an in depth-characterization of primary human synovial fibroblasts as an *ex vivo* model of CHIKV infection. Synovial fibroblasts have been described to be an aggressive key driver for rheumatoid arthritis by facilitating proinflammatory processes and stimulating the degradation of cartilage [26,27]. We found synovial fibroblasts to support the full replication cycle of CHIKV and characterized their intrinsic immune responses against CHIKV infection and their sensitivity to IFN exposure. Importantly, synovial fibroblasts from healthy donors and the more accessible synovial fibroblasts from osteoarthritic patients displayed very similar phenotypes in the context of CHIKV infection. Prospectively, this primary cell model provides the opportunity to address preclinical questions regarding the physiopathology of CHIKV.

Material and Methods

Cells and Viruses

Human osteosarcoma U2OS cells (a kind gift from T. Stradal, Hanover), human HEK293T cells (a kind gift from J. Bohne, Hanover), human foreskin fibroblast HFF-1 cell (ATTC-SCRC-1041) and hamster BHK-21 cells (ATCC CCL-10) were grown in Dulbecco's modified Eagle's medium - high glucose (DMEM, Sigma-Aldrich) supplemented with 10% heat-inactivated fetal bovine serum (FBS, Sigma-Aldrich), 2mM L-Glutamine (Gibco), and 100 units/ml penicillin-streptomycin (Gibco). Primary human fibroblasts were obtained from synovial biopsies from donors suffering from osteoarthritis (osteroarthrosis synovial fibroblasts, OASF) or a non-arthritic background (healthy donor synovial fibroblasts, HSF), purified, and cultured as described before [28]. The local ethic committee (Justus-Liebig-University Giessen) approved the cooperative study (ethical vote IDs 66-08 and 74-05). All patients gave written informed consent. Mycoplasma testing was routinely performed and negative in all primary human cell cultures. After 2-4 passages of initial cultivation, cells were used for experiments in high glucose DMEM supplemented with 20% FBS, 2 mM L-Glutamine, 100 units/ml penicillin-streptomycin, 1% non-essential amino acids (Gibco), and 1 % sodium pyruvate (Gibco). The CHIKV LR2006-OPY 5'GFP infectious clone expressing EGFP under the control of a subgenomic promotor (hereafter referred to as CHIKV) has been described previously [29]. Virus was produced by *in vitro*-transcription of and subsequent electroporation of RNA into BHK-21 cells. Virus-containing supernatant was collected, passaged once on BHK-21 cells and viral titers were determined by titration on HEK293T cells.

Infection, Treatments, Transfections

EGFP expression as surrogate for productive CHIKV infection was analyzed on a BD FACSCalibur, FACSLyric or Accuri C6. For neutralization assays, virus-containing supernatants were pre-incubated for one hour with anti-CHIKV E2 antibody C9 (Integral Molecular) at 1 µg/ml or with recombinant MXRA8-Fc (a kind gift from M. Diamond) at 150 ng/ml. Recombinant IFN-α2a (Roferon, Roche) and IFN-λ1 (Peprotech) was used where indicated. Transfections were performed using Lipofectamine2000 (Thermo Fisher) for plasmid DNA (pcDNA6 empty vector) or 5'triphosphate dsRNA (InvivoGen).

RNA-Seq Analysis

RNA was extracted using the Promega Maxwell 16 with LEV simplyRNA Tissue Kits. RNA quality was assessed using the Agilent Bioanalyzer and appropriate samples were used for NGS library preparation with the NEBNext Ultra II Directional RNA kit and sequenced with 50 bp paired-end reads and 30 mio reads per sample on the Illumina HiSeq 2500. Data was analyzed with CLC Genomics Workbench 12 (QIAGEN) by mapping the human reads onto the hg19 reference genome scaffold (GCA_000001405.28). Unmapped reads not matching the human genome were mapped onto the CHIKV genome LR2006_OPY (DQ443544.2). For HSF, infection and analysis were performed similarly, but RNA was extracted with the Zymo Research Direct-Zol RNA MiniPrep Kit, NGS libraries were prepared with the Illumina TruSeq stranded mRNA kit and sequencing was performed on the Illumina NextSeq500 with 65 mio reads per sample. Biological process enrichment was analyzed by Gene Ontology [30,31].

Results

Osteoarthritic fibroblasts are susceptible and permissive to CHIKV infection

First, we examined the capacity of primary human synovial fibroblasts to support the entire CHIKV replication cycle. Therefore, we infected synovial fibroblasts obtained from osteoarthritic patients (OASF) and from patients with a non-arthritic background (HSF) with CHIKV strain LR2006-OPY expressing EGFP under the control of a second subgenomic promotor. 24 hours post-infection, the proportion of EGFP-positive cells ranged between 4 and 24.5 % and did not differ between fibroblast types (Fig 1A). At the same time point, supernatants of both OASF and HSF displayed titers of 1.6-8.8x10^5 infectious particles per ml, with significantly higher titers produced by OASF. At 48 hours post-infection, virus titers produced by HSF did not further increase, whereas the titers produced by OASF reached up to 1.5x10^7 infectious particles per ml (Fig. 1B), suggesting slightly higher virus production and/or viral spread in OASF as compared to HSF.

Susceptibility of cells to CHIKV infection is enhanced by the attachment factor MXRA8 [10]. Similarly, the cytosolic protein FHL-1 is essential for CHIKV genome replication [11]. We confirmed the expression of these two cellular cofactors in OASF and HSF by immunoblotting and/or immunofluorescence (Fig. 1C). We assessed the functional relevance of the MXRA8 attachment factor using a soluble MXRA8-Fc fusion protein, which blocks the binding site on the E1-E2 glycoprotein complex on the virus surface [10,32]. At a low MOI, MXRA8-Fc-preincubated CHIKV was 50 % less infectious to synovial fibroblasts, and this inhibition was reversed when saturating amounts of infectious virus particles were used (Fig. 1D), indicating that endogenous MXRA8 may contribute, at least partially, to CHIKV entry in OASF.

We next wondered whether IL-1β-mediated activation of synovial fibroblasts, a hallmark of rheumatoid arthritis [33-35], modulates their susceptibility to CHIKV infection. Treatment with IL-1β, while readily inducing IL-6 secretion, did not alter the percentage of EGFP-positive cells upon CHIKV challenge (Fig. 1E). Conversely, infection with CHIKV induced very mild secretion of IL-6 only at 48 hours post-infection, and did not modulate the amount of IL-6 secreted upon IL-1β treatment (Fig. 1F). These data suggest that CHIKV infection of synovial fibroblasts neither induces nor modulates IL-6 secretion, arguing against their activation.

To determine the importance of IFN-mediated antiviral immunity in this primary cell system, we monitored the infection in the absence or presence of the JAK/STAT inhibitor Ruxolitinib. Using live-cell imaging, we documented the increase in EGFP-positive cells between ten and 48 hours post-infection, which progressed faster in Ruxolitinib-treated cultures, and an onset of cytopathic effects after 24 hours in all infected cultures (Fig. 1G, Suppl. Mov. M1). Analysis of the EGFP intensity in each frame over time confirmed the higher expression of EGFP in Ruxolitinib-treated cultures (Fig. 1H, Suppl. Mov. M2). To assess the ability of CHIKV to persist in a fibroblast cultures over multiple passages, virus-containing supernatants of infected OASF were transferred to an uninfected culture, in the presence or absence of Ruxolitinib. The initial infection rates were markedly higher in Ruxolitinib-treated cultures (18.6 times on average), however, EGFP positivity was lost after two to three passages (Fig. 1I). Overall, these experiments establish the susceptibility and permissiveness of synovial fibroblasts to CHIKV infection and their expression of important cellular cofactors. Furthermore, we showed an absence of interconnection between IL1-β activation and susceptibility to infection, and restriction of infection through JAK/STAT-mediated innate immunity.

Productive CHIKV infection provokes a strong cell-intrinsic immune response in OASF

Next, we performed RNA-seq analysis on OASF infected with CHIKV, in the absence or presence of the E2-binding, neutralizing antibody C9 [36], and on mock-infected cells. C9 pre-treatment resulted in potent inhibition of the infection by (Fig. 2A). Upon CHIKV infection, expression of numerous interferon-stimulated genes (ISGs) was induced at the protein level in a C9 treatment-sensitive manner, including IFITM3, ISG15, and MX2. As expected, production of the viral E1-E2 and Capsid proteins was detectable specifically in CHIKV-infected, but not in cells exposed to C9-pretreated virus (Fig. 2B). We performed global transcriptional profiling of mock- and CHIKV-infected OASF by RNA-Seq and identified 992 significantly up- and 99 significantly downregulated genes in CHIKV-infected cells 24 hours post-infection (Fig. 2C). No significant differences were observed between the transcriptional profiles of uninfected cells and cells exposed to C9-treated virus (data not shown). We defined a set of prototype effector genes of the cell-intrinsic immune response, such as ISGs and proinflammatory transcription factors. Most of these genes were highly upregulated in CHIKV-infected cells, demonstrating a broad and strong activation of antiviral immune responses (Fig. 2D) in cells from four different donors with no statistically significant deviation in the magnitude of induction. Upon CHIKV infection, upregulation of *IFNB* and *IFNL1*, *IFNL2*, and *IFNL3* expression was statistically significant but low in magnitude. Almost no *IFNA* mRNA was upregulated upon CHIKV infection. Expression of mRNAs for all IFN receptors was detectable and stable with exception of the IFN-λ receptor, which was upregulated upon CHIKV infection. Established host factors for CHIKV as well as fibroblast marker genes and cellular housekeeping genes were not quantitatively altered in their expression. Virtual absence of expression of monocyte/macrophage lineage-specific genes excluded the possibility of a contamination of the fibroblast culture with macrophages, which occasionally has been reported in early passages of *ex vivo* cultured synovial

fibroblasts [28] (Fig. 2D). In productively infected cultures, 19-54 % of the reads were attributed to the CHIKV genome (Fig. 2E). Additionally, the 26S subgenomic viral RNA was 10-fold more abundant than nonstructural subgenomes in both CHIKV-infected cells and cells inoculated with C9-neutralized virus (Fig. 2F). Overall, CHIKV-infected OASF sense and react to productive CHIKV infection with the extensive upregulation of antiviral and proinflammatory ISGs. Interferon expression itself was low at 24 hours post-infection, not excluding the possibility that it peaked transiently at earlier time points.

HSF and OASF share a similar base-line and CHIKV-induced transcriptome

We next aimed at uncovering potential differences between fibroblasts from donors with different clinical conditions. In fibroblasts from healthy donors, infection rates, the resulting immune response, and the ratio of human and CHIKV RNAs equaled those of OASF (Fig. S1). A potential transcriptional predisposition in the cells of either category was largely excluded by the finding of a good correlation of the gene expression profile of respective uninfected samples (R^2=0.9086) (Fig. 3A). The CHIKV-inducible program of genes was not significantly differentially dysregulated at baseline when comparing uninfected OASF and HSF cells. Indeed, the pathways in which the differentially expressed genes were involved in were mostly part of organ development and cellular regulatory processes, and not of inflammatory or antiviral processes (Fig. 3B). Additionally, the transcriptional profile in CHIKV-infected OASF and HSF displayed a similarly good correlation of the gene expression (R^2=0.9085, Fig. 3C), with an equivalently strong upregulation of prototypic inflammation genes (R^2=0.7565, Fig. 3D). Interestingly, the number of genes significantly up- and downregulated upon CHIKV infection was 1.23-fold and 3.57-fold higher in HSF compared to OASF, respectively, but 55.4% of upregulated genes from both groups overlapped (Fig. 3E). Gene ontology analysis of the upregulated genes in HSF identified

pathways similar to those seen in OASF, such as the response to interferons and viruses, cytokine-mediated processes, and cell-intrinsic defense mechanisms (Fig. 3F). Conclusively, OASF and HSF share similar basal and CHIKV-inducible transcriptional profiles. Minor differences were present only in gene families not linked to innate immunity, while important mediators of antiviral immunity were equally strongly upregulated upon CHIKV infection in both OASF and HSF.

The cell-intrinsic response to CHIKV infection in primary synovial fibroblasts exceeds the one induced in immortalized cell lines

We noticed that infection rates in OASF rarely increased after 24 hours post-infection, and suspected this to be the result of the strong immune activation and subsequent IFN signaling. As a reference, the commonly used osteosarcoma cell line U2OS was much more susceptible to CHIKV infection. As an additional reference, HFF-1, an immortalized fibroblast cell line, displayed reduced susceptibility (Fig. 4A). OASF exhibited very strong ISG responses, which exceeded those mounted by U2OS and HFF-1 cells at both 24 and 48 hours post-infection (Fig. 4B). To exclude the possibility that cell lines are less able to sense viral RNA, we performed stimulation experiments with a 5'-triphosphate dsRNA (5-ppp-RNA), which exclusively stimulates the RNA sensor RIG-I [37], the main sensor of CHIKV RNA in infected cells [38] (Fig. 4C). Because of the reported involvement of the DNA sensor cGAS in modulating RNA-viral infections [39-42], we further tested the ability of all cell types to sense plasmid DNA (Fig. 4D). All cell types responded to stimulation with 5-ppp-RNA and DNA by upregulating *IFIT1* and *MX2* mRNA. There was a trend towards strongest responses in OASF, despite the absence of statistical significance between the individual three cell systems. These findings demonstrate that even though the response to a virus-independent, specific stimulus led to immune responses of largely similar magnitudes in all cultured cells,

the response to the viral infection was highest in the primary synovial fibroblasts. This may reflect a synovial fibroblast-specific response to CHIKV infection and/or inefficiency of viral antagonism of host defenses.

Primary synovial fibroblast-specific sensitivities to type I and III IFN treatment

Type I and III IFNs play a crucial role in limiting virus infection and protecting the host [43-45]. Here, we analyzed to what extent they restrict CHIKV infection in OASF. Furthermore, we quantified the corresponding induction of expression of *IFIT1* and *MX2* mRNAs as surrogates for the overall response to IFN treatment. First, we pre-stimulated OASF individually with a range of IFN-α2a and –λ1 concentrations for 48 h and infected the cells with CHIKV in the continuous presence of the IFNs. All investigated concentrations, even the lowest dose, of IFN-α almost completely inhibited CHIKV infection. In contrast, IFN-λ inhibited infection less efficiently, in a largely dose-dependent fashion (Fig. 5A, left panel). The antiviral state induced by IFN-α pre-treatment manifested itself by a robust and dose-dependent *IFIT1* and *MX2* mRNA expression at the time point of infection initiation. IFN-λ pre-treatment mediated a comparably lower and less dose-dependent induction of ISGs (Fig. S2A, left panel). Additionally, we investigated IFN-α in a post-infection treatment setting (Post-treatment). When added four hours post-infection, IFN-α still displayed a clear, though less potent antiviral activity when compared to the pre-treatment setting (Fig. 5A, right panel). In parallel to the assessment of antiviral activity, we quantified the antiviral state induced by either the IFN treatment alone, or the state resulting from the combination of infection and subsequent IFN post-treatment. Interestingly, a preceding CHIKV infection failed to prevent ISG induction, and led to expression levels of *IFIT1* and *MX2* even exceeding those induced by IFN-α (Fig. S2). These data are in contrast to previous reports of efficient CHIKV-mediated antagonism of IFN signaling in Vero cell lines [15].

Analogous experiments in U2OS and HFF-1 cells yielded partially different outcomes. Although less effective than in OASF, IFN-α pre-treatment restricted CHIKV infection both in U2OS and HFF-1 cells, despite more efficient IFN-α induced expression of *IFIT1* and *MX2* in U2OS cells when compared to HFF-1, suggesting different abilities of the two cell lines to exert ISG-mediated antiviral restriction. IFN-λ pre-treatment was more potent in U2OS cells than in OASF, and largely ineffective in HFF-1 cells (Fig. 5B, left panels). IFN-λ antiviral activity in U2OS cells was accompanied by a decent expression of ISG mRNAs (Fig. S2B, left panel). In HFF-1 cells, a lack of IFN-λ antiviral activity correlated with a weak induction of *IFIT1* and *MX2* mRNA expression, which was in the same range as those detected in OASF and which was sufficient to exert an antiviral effect, pointing to different efficiencies of a given antiviral state in the two cell systems (Fig. 5B, left panels). Post-treatment of both immortalized cell lines with IFN-α was very ineffective (Fig. 5B, C, right panels), even though we observed a dose-dependent ISG induction in both cells lines (Fig. S2B, C, right panels). Overall, the data suggest a stronger sensitivity of OASF to IFN-α-induced immunity compared to commonly used immortalized cell lines. IFN-λ pre-treatment of OASF, although not as effective as in the osteosarcoma cell line U2OS, clearly inhibited CHIKV infection, suggesting that these primary synovial fibroblasts express levels of IFN-λ receptors that are sufficient to signal upon IFN-λ treatment. This corresponds to our observation that the *IFNLR1* gene is not only expressed, but upregulated in CHIKV infected OASF (Fig. 2D). Most interestingly, and in striking contrast to the immortalized cell lines, OASF were unique in their ability to transform a post-infection treatment of IFN-α into a relatively potent antiviral program, suggesting that postulated virus-mediated antagonistic strategies against IFNs such as the inhibition of STAT1 nuclear translocation or a host transcriptional and translational shutoff [15-17,46,47] are poorly effective in primary synovial fibroblasts. Collectively, these data uncover crucial differences between primary synovial fibroblasts and

widely used immortalized cell lines and underline the need to study virus-host interactions in primary target cells of CHIKV infection.

Discussion

Considering the CHIKV-induced arthritis, it is likely that cells of the synovium are directly implicated in the pathophysiology of CHIKV infection. Cells of the synovial tissue and synovial fluid contain CHIKV RNA and protein upon CHIKV infection *in vivo* in humans [7], experimentally infected macaques [48], and mice [49]. The main cell types composing the synovium are macrophages and fibroblasts. The latter have been identified to be susceptible to CHIKV infection *ex vivo* [10,50,51]. However, the corresponding basal innate immune state of primary synovial fibroblasts and their ability to exert IFN-mediated antiviral restriction is unknown. Here, we establish that the widely available OASF and less available HSF share susceptibility and permissiveness to CHIKV infection and their basal and infection-induced transcriptional program. These findings are in line with reports on overall transcriptional similarity of the two cell types, except in some signaling pathways unrelated to immunity [52]. CHIKV infection provoked a striking cellular response that involves upregulation of multiple ISGs, many of them exerting antiviral activity. Although we did not define the PAMP(s) that trigger responses in synovial macrophages, infection by alphaviruses typically raises RIG-I-mediated responses through exposure of dsRNA intermediates and provokes mitochondrial DNA leakage that is sensed via cGAS/STING [38,39,41]. Indeed, experimental ligands of both sensors were highly reactive in OASF, as was IFN-α pre-treatment. Surprisingly, also IFN-λ pre-treatment translated into an antiviral state, indicating that synovial fibroblasts may represent an exception to the notion of otherwise IFN-λ-nonresponsive fibroblasts [53]. Finally, CHIKV infection of synovial fibroblasts was sensitive to IFN-α applied after inoculation with virus. These findings appear to contrast potent virus-mediated antagonism of IFN in U2OS and HFF-1 cell lines, which has been suggested to involve counteraction of nuclear translocation of STAT1 [15,16]. Also, unaltered levels of expression of housekeeping genes and genes encoding fibroblast markers did not generate

evidence for virus-mediated host transcriptional shut-off reported in several cell lines [17,18]. Overall, synovial fibroblasts appear to react differently to CHIKV as compared to commonly used cell lines, and to be particularly responsive to CHIKV infection. The underlying reason for this difference is unknown, but may involve a different intracellular milieu that is hyper-responsive to CHIKV infection. Future studies are required to delineate the exact mode of CHIKV sensing in productively infected synovial fibroblasts. In addition, it will be important to study the impact of potential abortive infection events, occurring either due to uptake of defective interfering particles and/or due to high refractoriness of individual cells, to the overall cellular response in an infected culture or tissue. Finally, the interplay of tissue-resident, synovial macrophages and fibroblasts likely additionally modulates CHIKV infection and cellular responses.

It is tempting to speculate that the synovial fibroblast-specific hyperreactivity is linked to the long-term arthralgia observed *in vivo* in chronic CHIKV patients, and that pharmacological interference with hyperinflammation represents a feasible intervention approach towards alleviation of long-term arthralgia. In rheumatoid arthritis, hyperactivated synovial fibroblasts are known to invade the joint matrix, destroying/disrupting the cartilage and causing long-term inflammation [26,54]. This and the subsequent attraction of immune cells, including monocyte-derived macrophages to the damaged sites, may represent important events in the progression to long-term morbidity [55]. Indeed, data obtained in recent clinical studies suggest that treatment of chikungunya-induced arthritis with the immunosuppressant methotrexate may be a beneficial strategy [56,57].

Acknowledgements

We thank the sequencing core of the Helmholtz Centre for Infection Research (HZI) and the Genomics platform of the Berlin Institute of Health (BIH) for preparation of the Illumina sequencing libraries and the next generation sequencing. We thank M. Diamond for providing the MXRA8-Fc proteins. We thank Theresia Stradal and Jens Bohne for providing U2OS cells and HEK293T cells, respectively. We thank Christian Drosten for constant support. This work was supported by funding from Deutsche Forschungsgemeinschaft (DFG) to C.G. (GO2153/3-1), by the Impulse and Networking Fund of the Helmholtz Association through the HGF-EU partnering grant PIE-008 to C.G., and by funding from the Helmholtz Center for Infection Research (HZI) and Berlin Institute of Health (BIH) to C.G.

Declaration of Interest

The authors declare they have no actual or potential competing financial interests.

References

1. Matusali G, Colavita F, Bordi L, et al. Tropism of the Chikungunya Virus. Viruses. 2019 Feb 20;11(2).
2. Levi LI, Vignuzzi M. Arthritogenic Alphaviruses: A Worldwide Emerging Threat? Microorganisms. Vol. 72019.
3. Couderc T, Lecuit M. Chikungunya virus pathogenesis: From bedside to bench. Antiviral research. 2015 Sep;121:120-31.
4. Paixao ES, Rodrigues LC, Costa M, et al. Chikungunya chronic disease: a systematic review and meta-analysis. Trans R Soc Trop Med Hyg. 2018 Jul 1;112(7):301-316.
5. Suhrbier A. Rheumatic manifestations of chikungunya: emerging concepts and interventions. Nat Rev Rheumatol. 2019 Oct;15(10):597-611.
6. Chow A, Her Z, Ong EK, et al. Persistent arthralgia induced by Chikungunya virus infection is associated with interleukin-6 and granulocyte macrophage colony-stimulating factor. The Journal of infectious diseases. 2011 Jan 15;203(2):149-57.
7. Hoarau JJ, Jaffar Bandjee MC, Krejbich Trotot P, et al. Persistent chronic inflammation and infection by Chikungunya arthritogenic alphavirus in spite of a robust host immune response. J Immunol. 2010 May 15;184(10):5914-27.

8. Young AR, Locke MC, Cook LE, et al. Dermal and muscle fibroblasts and skeletal myofibers survive chikungunya virus infection and harbor persistent RNA. PLoS pathogens. 2019 Aug;15(8):e1007993.
9. Chang AY, Martins KAO, Encinales L, et al. Chikungunya Arthritis Mechanisms in the Americas: A Cross-Sectional Analysis of Chikungunya Arthritis Patients Twenty-Two Months After Infection Demonstrating No Detectable Viral Persistence in Synovial Fluid. Arthritis & rheumatology (Hoboken, NJ). 2018 Apr;70(4):585-593.
10. Zhang R, Kim AS, Fox JM, et al. Mxra8 is a receptor for multiple arthritogenic alphaviruses. Nature. 2018 May;557(7706):570-574.
11. Meertens L, Hafirassou ML, Couderc T, et al. FHL1 is a major host factor for chikungunya virus infection. Nature. 2019 Sep 25.
12. Salvador B, Zhou Y, Michault A, et al. Characterization of Chikungunya pseudotyped viruses: Identification of refractory cell lines and demonstration of cellular tropism differences mediated by mutations in E1 glycoprotein. Virology. 2009 Oct 10;393(1):33-41.
13. Reynaud JM, Kim DY, Atasheva S, et al. IFIT1 Differentially Interferes with Translation and Replication of Alphavirus Genomes and Promotes Induction of Type I Interferon. PLoS pathogens. 2015 Apr;11(4):e1004863.
14. Poddar S, Hyde JL, Gorman MJ, et al. The Interferon-Stimulated Gene IFITM3 Restricts Infection and Pathogenesis of Arthritogenic and Encephalitic Alphaviruses. Journal of virology. 2016 Oct 1;90(19):8780-94.
15. Fros JJ, Liu WJ, Prow NA, et al. Chikungunya virus nonstructural protein 2 inhibits type I/II interferon-stimulated JAK-STAT signaling. Journal of virology. 2010 Oct;84(20):10877-87.
16. Goertz GP, McNally KL, Robertson SJ, et al. The Methyltransferase-Like Domain of Chikungunya Virus nsP2 Inhibits the Interferon Response by Promoting the Nuclear Export of STAT1. Journal of virology. 2018 Sep 1;92(17).
17. Akhrymuk I, Kulemzin SV, Frolova EI. Evasion of the innate immune response: the Old World alphavirus nsP2 protein induces rapid degradation of Rpb1, a catalytic subunit of RNA polymerase II. Journal of virology. 2012 Jul;86(13):7180-91.
18. Akhrymuk I, Lukash T, Frolov I, et al. Novel Mutations in nsP2 Abolish Chikungunya Virus-Induced Transcriptional Shutoff and Make the Virus Less Cytopathic without Affecting Its Replication Rates. Journal of virology. 2019 Feb 15;93(4).
19. Haese NN, Broeckel RM, Hawman DW, et al. Animal Models of Chikungunya Virus Infection and Disease. The Journal of infectious diseases. 2016 Dec 15;214(suppl 5):S482-s487.
20. Simarmata D, Ng DC, Kam YW, et al. Early clearance of Chikungunya virus in children is associated with a strong innate immune response. Scientific reports. 2016 May 16;6:26097.
21. Schilte C, Couderc T, Chretien F, et al. Type I IFN controls chikungunya virus via its action on nonhematopoietic cells. J Exp Med. 2010 Feb 15;207(2):429-42.
22. Soares-Schanoski A, Baptista Cruz N, de Castro-Jorge LA, et al. Systems analysis of subjects acutely infected with the Chikungunya virus. PLoS pathogens. 2019 Jun;15(6):e1007880.
23. Hussain KM, Lee RC, Ng MM, et al. Establishment of a Novel Primary Human Skeletal Myoblast Cellular Model for Chikungunya Virus Infection and Pathogenesis. Scientific reports. 2016 Feb 19;6:21406.
24. Sukkaew A, Thanagith M, Thongsakulprasert T, et al. Heterogeneity of clinical isolates of chikungunya virus and its impact on the responses of primary human fibroblast-like synoviocytes. J Gen Virol. 2018 Apr;99(4):525-535.

25. Bernard E, Hamel R, Neyret A, et al. Human keratinocytes restrict chikungunya virus replication at a post-fusion step. Virology. 2015 Feb;476:1-10.
26. Neumann E, Lefevre S, Zimmermann B, et al. Rheumatoid arthritis progression mediated by activated synovial fibroblasts. Trends Mol Med. 2010 Oct;16(10):458-68.
27. Lefevre S, Meier FM, Neumann E, et al. Role of synovial fibroblasts in rheumatoid arthritis. Curr Pharm Des. 2015;21(2):130-41.
28. Neumann E, Riepl B, Knedla A, et al. Cell culture and passaging alters gene expression pattern and proliferation rate in rheumatoid arthritis synovial fibroblasts. Arthritis research & therapy. 2010;12(3):R83.
29. Tsetsarkin K, Higgs S, McGee CE, et al. Infectious clones of Chikungunya virus (La Reunion isolate) for vector competence studies. Vector borne and zoonotic diseases (Larchmont, NY). 2006 Winter;6(4):325-37.
30. The Gene Ontology Resource: 20 years and still GOing strong. Nucleic Acids Res. 2019 Jan 8;47(D1):D330-d338.
31. Ashburner M, Ball CA, Blake JA, et al. Gene ontology: tool for the unification of biology. The Gene Ontology Consortium. Nat Genet. 2000 May;25(1):25-9.
32. Basore K, Department of Pathology & Immunology WUSoM, Saint Louis, MO 63110, USA, Kim AS, et al. Cryo-EM Structure of Chikungunya Virus in Complex with the Mxra8 Receptor. Cell. 2019;0(0).
33. Georganas C, Liu H, Perlman H, et al. Regulation of IL-6 and IL-8 expression in rheumatoid arthritis synovial fibroblasts: the dominant role for NF-kappa B but not C/EBP beta or c-Jun. J Immunol. 2000 Dec 15;165(12):7199-206.
34. Gitter BD, Labus JM, Lees SL, et al. Characteristics of human synovial fibroblast activation by IL-1 beta and TNF alpha. Immunology. 1989 Feb;66(2):196-200.
35. Kay J, Calabrese L. The role of interleukin-1 in the pathogenesis of rheumatoid arthritis. Rheumatology (Oxford). 2004 Jun;43 Suppl 3:iii2-iii9.
36. Selvarajah S, Sexton NR, Kahle KM, et al. A neutralizing monoclonal antibody targeting the acid-sensitive region in chikungunya virus E2 protects from disease. PLoS neglected tropical diseases. 2013;7(9):e2423.
37. Hornung V, Ellegast J, Kim S, et al. 5'-Triphosphate RNA is the ligand for RIG-I. Science (New York, NY). 2006 Nov 10;314(5801):994-7.
38. Sanchez David RY, Combredet C, Sismeiro O, et al. Comparative analysis of viral RNA signatures on different RIG-I-like receptors. eLife. 2016 Mar 24;5:e11275.
39. Schoggins JW, MacDuff DA, Imanaka N, et al. Pan-viral specificity of IFN-induced genes reveals new roles for cGAS in innate immunity. Nature. 2014 Jan 30;505(7485):691-5.
40. Zheng Y, Liu Q, Wu Y, et al. Zika virus elicits inflammation to evade antiviral response by cleaving cGAS via NS1-caspase-1 axis. Embo j. 2018 Sep 14;37(18).
41. Aguirre S, Luthra P, Sanchez-Aparicio MT, et al. Dengue virus NS2B protein targets cGAS for degradation and prevents mitochondrial DNA sensing during infection. Nature microbiology. 2017 Mar 27;2:17037.
42. Parker MT, Gopinath S, Perez CE, et al. Innate Immune Priming by cGAS as a Preparatory Countermeasure Against RNA Virus Infection. bioRxiv. 2018:434027.
43. Lazear HM, Schoggins JW, Diamond MS. Shared and Distinct Functions of Type I and Type III Interferons. Immunity. 2019 Apr 16;50(4):907-923.
44. Schoggins JW, Wilson SJ, Panis M, et al. A diverse range of gene products are effectors of the type I interferon antiviral response. Nature. 2011 Apr 28;472(7344):481-5.
45. Zhou JH, Wang YN, Chang QY, et al. Type III Interferons in Viral Infection and Antiviral Immunity. Cell Physiol Biochem. 2018;51(1):173-185.

46. White LK, Sali T, Alvarado D, et al. Chikungunya virus induces IPS-1-dependent innate immune activation and protein kinase R-independent translational shutoff. Journal of virology. 2011 Jan;85(1):606-20.
47. Bae S, Lee JY, Myoung J. Chikungunya Virus-Encoded nsP2, E2 and E1 Strongly Antagonize the Interferon-beta Signaling Pathway. J Microbiol Biotechnol. 2019 Nov 28;29(11):1852-1859.
48. Labadie K, Larcher T, Joubert C, et al. Chikungunya disease in nonhuman primates involves long-term viral persistence in macrophages. J Clin Invest. 2010 Mar;120(3):894-906.
49. Couderc T, Chrétien F, Schilte C, et al. A mouse model for Chikungunya: young age and inefficient type-I interferon signaling are risk factors for severe disease. PLoS pathogens. 2008 Feb 8;4(2):e29.
50. Agrawal M, Pandey N, Rastogi M, et al. Chikungunya virus modulates the miRNA expression patterns in human synovial fibroblasts. J Med Virol. 2020 Feb;92(2):139-148.
51. Selvamani SP, Mishra R, Singh SK. Chikungunya virus exploits miR-146a to regulate NF-κB pathway in human synovial fibroblasts. PloS one. 2014;9(8):e103624.
52. Del Rey MJ, Usategui A, Izquierdo E, et al. Transcriptome analysis reveals specific changes in osteoarthritis synovial fibroblasts. Annals of the rheumatic diseases. 2012 Feb;71(2):275-80.
53. Sommereyns C, Paul S, Staeheli P, et al. IFN-lambda (IFN-lambda) is expressed in a tissue-dependent fashion and primarily acts on epithelial cells in vivo. PLoS pathogens. 2008 Mar 14;4(3):e1000017.
54. Hillen J, Geyer C, Heitzmann M, et al. Structural cartilage damage attracts circulating rheumatoid arthritis synovial fibroblasts into affected joints. Arthritis research & therapy. 2017 Feb 28;19(1):40.
55. Falconer J, Murphy AN, Young SP, et al. Review: Synovial Cell Metabolism and Chronic Inflammation in Rheumatoid Arthritis. Arthritis & rheumatology (Hoboken, NJ). 2018 Jul;70(7):984-999.
56. Amaral JK, Sutaria R, Schoen RT. Treatment of Chronic Chikungunya Arthritis With Methotrexate: A Systematic Review. Arthritis Care Res (Hoboken). 2018 Oct;70(10):1501-1508.
57. Ganu MA, Ganu AS. Post-chikungunya chronic arthritis--our experience with DMARDs over two year follow up. J Assoc Physicians India. 2011 Feb;59:83-6.

Legends

Figure 1. Osteoarthritis fibroblasts are susceptible and permissive to CHIKV infection. **(A)** OASF or HSF were infected with 5'EGFP-CHIKV (MOI 10). Tthe percentage of EGFP-positive cells was quantified by flow cytometry (n = 12 for OASF, 5 for HSF. Values are derived from data also shown in Fig. 2, 5, and S1). **(B)** Supernatants of CHIKV-infected OASF were collected at 24 and 48 hpi, titrated on HEK293T cells, and titers were determined by analyzing EGFP expression at 24 hpi. For background controls (post-wash), samples were collected 1 h post virus inoculation and subsequent washing (n = 3). **(C)** Uninfected OASF and HSF were analyzed for MXRA8 and FHL1 expression by immunoblotting (n = 4-6) and for MXRA8 expression by immunofluorescence. Scale bar = 50 µm (n = 3, representative images shown). **(D)** OASF were infected with 5'EGFP-CHIKV treated with MXRA8-Fc recombinant protein or mock-treated virus. At 24 hpi, cells were analyzed for EGFP expression (n = 4). **(E)** OASF were stimulated with IL-1β at 10 ng/ml for 16 h and subsequently infected with CHIKV (MOI 10) in the presence of IL-1β. Mock-stimulated OASF were infected as a control. Cells were analyzed for EGFP expression and **(F)** supernatant was analyzed for IL-6 secretion by ELISA (n = 3). **(G)** OASF were infected with 5'EGFP-CHIKV (MOI 10) in the absence or presence of Ruxolitinib (10 µM) or mock-infected. Infection was analyzed by live-cell imaging and representative images are shown. Scale bar = 100 µm (n = 3). **(H)** Live-cell imaging from G was analyzed for EGFP intensity using ImageJ. **(I)** OASF were treated with Ruxolitinib or mock-treated for 16 h, infected with 5'EGFP-CHIKV (MOI 10) and supernatant was transferred to uninfected, untreated or Ruxolitinib-pretreated OASF every two to three days. Expression of EGFP in the target cells was quantified at indicated time points (n = 3).

Figure 2. Productive CHIKV infection provokes a strong cell-intrinsic immune response in OASF.

(A) OASF were infected with 5'EGFP-CHIKV (MOI 10) in the presence or absence of the anti-E2 antibody C9. At 24 hpi, the percentage of EGFP-positive cells was measured by flow cytometry (filled squares: donor cells used for RNA-seq, n = 4. Values shown for comparison are derived from data plotted in Fig. 5). **(B)** Immunoblot of selected proteins expressed upon infection in samples from A (n = 4). **(C-F)** RNA from cells infected in A was extracted and subjected to RNA-seq (n = 4). **(C)** Analysis of up- and downregulated genes in CHIKV-infected samples compared to mock infection. Dotted lines indicate cutoff for <1.5 fold regulation and a p-value of 0.05. **(D)** Heatmaps of selected gene expression profiles related to innate immune responses (left) or to secreted proinflammatory mediators (middle) as well as to the expression of interferon receptors, CHIKV cofactors, and cellular expression markers (right) in uninfected or CHIKV-infected cells. **(E)** Number of NGS reads attributed to the human or CHIKV reference genome in CHIKV or neutralizing antibody-treated CHIKV infected cells. **(F)** NGS reads attributed to each individual position in the CHIKV genome plotted for cells infected with CHIKV in the presence or absence of neutralizing antibody. SGP: subgenomic promotor-

Figure 3. HSF and OASF share a similar base-line and CHIKV-induced transcriptome.

(A) Visualization of global transcriptional differences between OASF and HSF under regular culturing conditions. Average RPKM ($\log_{10}$) values for all detected transcripts from OASF are plotted on the x-axis, with corresponding values from HSF plotted on the y-axis. R^2 value and regression line for comparison are inset. **(B)** Gene ontology analysis of differentially expressed genes in OASF compared to HSF. **(C)** Visualization of global transcriptomic differences between CHIKV-infected OASF and HSF as described in A. **(D)** Visualization of

the fold change induction of indicated genes in CHIKV-infected OASF and HSF. Average fold change (log_2) values for infected OASF are plotted on the x-axis, with corresponding values from infected HSF plotted on the y-axis. R^2 value and regression line for the comparison are inset. **(E)** Overlap of significantly (FDR-p <0.05) up- and downregulated genes in infected OASF and HSF. Numbers of genes up- or downregulated in either OASF or HSF only, or in both cell-types, are indicated. **(F)** Gene ontology analysis of the top significantly upregulated pathways in OASF, HSF, and shared by both in response to CHIKV infection.

Figure 4. The cell-intrinsic response to CHIKV infection in primary synovial fibroblasts exceeds the one induced in immortalized cell lines.

(A) OASF and HFF-1 cells were infected (MOI 10), U2OS cells were infected (MOI 0.5), and EGFP-positive cells were quantified by flow cytometry (n = 3-6). **(B)** Cells infected in A were analyzed for expression of *IFIT1* and *MX2* mRNA by quantitative RT-PCR (n = 3-6). Data from (A) and (B) is derived from experiments shown in Fig. 5. **(C)** Indicated cell cultures were transfected with 5'-triphosphate dsRNA (5-ppp-RNA) and analyzed for the expression of *IFIT1* (left) and *MX2* (right) mRNA (n = 3-4) **(D)** Same as F, but with plasmid DNA as transfectant (n = 3).

Figure 5. Primary synovial fibroblast-specific sensitivities to type I and III IFN treatment

(A) For a pre-treatment setting, OASF were treated with IFN-α2a or –λ1 for 48 h before infection with 5'EGFP-CHIKV (MOI 10) in the presence of IFN (left panel). For a post-treatment setting, OASF were infected with 5'-EGFP CHIKV (MOI 10) and IFN-α2a was

added 4 hpi (right panel). EGFP-positive cells were quantified by flow cytometry. **(B)** U2OS cells were treated and analyzed as described in (A), but infected at an MOI of 0.5. **(C)** HFF-1 cells were treated, infected, and analyzed as described in (A). UT: untreated (n = 3 for all experiments)

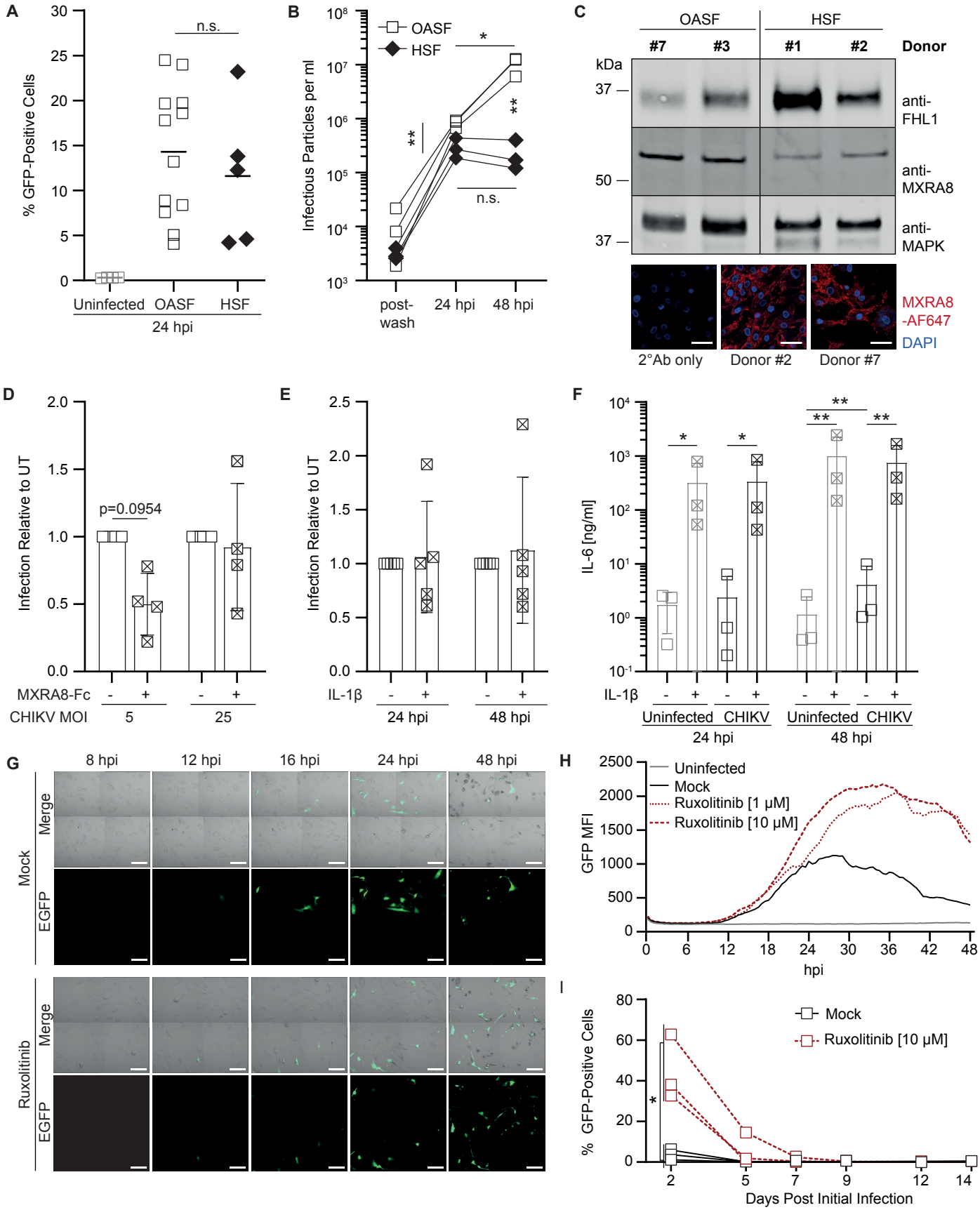
A
% GFP-Positive Cells
n.s.
Uninfected
OASF
HSF
24 hpi
B
Infectious Particles per ml
OASF
HSF
post-wash
24 hpi
48 hpi
n.s.
C
OASF
HSF
#7
#3
#1
#2
Donor
kDa
37
50
37
anti-FHL1
anti-MXRA8
anti-MAPK
MXRA8-AF647
DAPI
2°Ab only
Donor #2
Donor #7
D
Infection Relative to UT
p=0.0954
MXRA8-Fc
CHIKV MOI
5
25
E
Infection Relative to UT
IL-1β
24 hpi
48 hpi
F
IL-6 [ng/ml]
IL-1β
Uninfected
CHIKV
24 hpi
48 hpi
G
8 hpi
12 hpi
16 hpi
24 hpi
48 hpi
Mock
Ruxolitinib
Merge
EGFP
H
GFP MFI
Uninfected
Mock
Ruxolitinib [1 μM]
Ruxolitinib [10 μM]
hpi
I
% GFP-Positive Cells
Mock
Ruxolitinib [10 μM]
Days Post Initial Infection

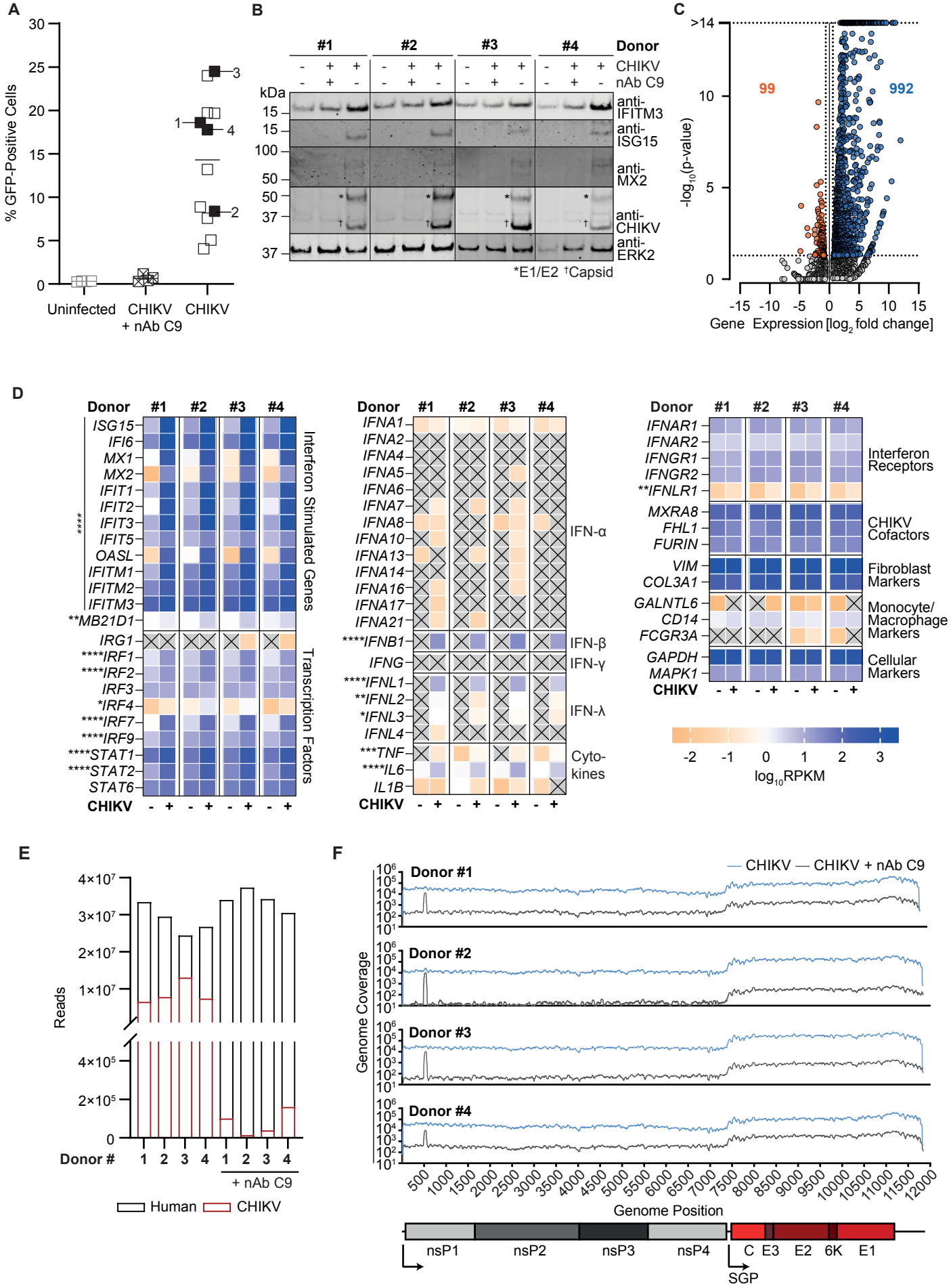
A
% GFP-Positive Cells
Uninfected
CHIKV
CHIKV + nAb C9
B
Donor
#1
#2
#3
#4
CHIKV
nAb C9
kDa
anti-IFITM3
anti-ISG15
anti-MX2
anti-CHIKV
anti-ERK2
*E1/E2 †Capsid
C
-log10(p-value)
99
992
Gene Expression [log2 fold change]
D
Interferon Stimulated Genes
Transcription Factors
IFN-α
IFN-β
IFN-γ
IFN-λ
Cyto-kines
Interferon Receptors
CHIKV Cofactors
Fibroblast Markers
Monocyte/ Macrophage Markers
Cellular Markers
log10RPKM
E
Reads
Donor #
+ nAb C9
Human
CHIKV
F
Donor #1
Donor #2
Donor #3
Donor #4
CHIKV
CHIKV + nAb C9
Genome Coverage
Genome Position
nsP1
nsP2
nsP3
nsP4
C
E3
E2
6K
E1
SGP

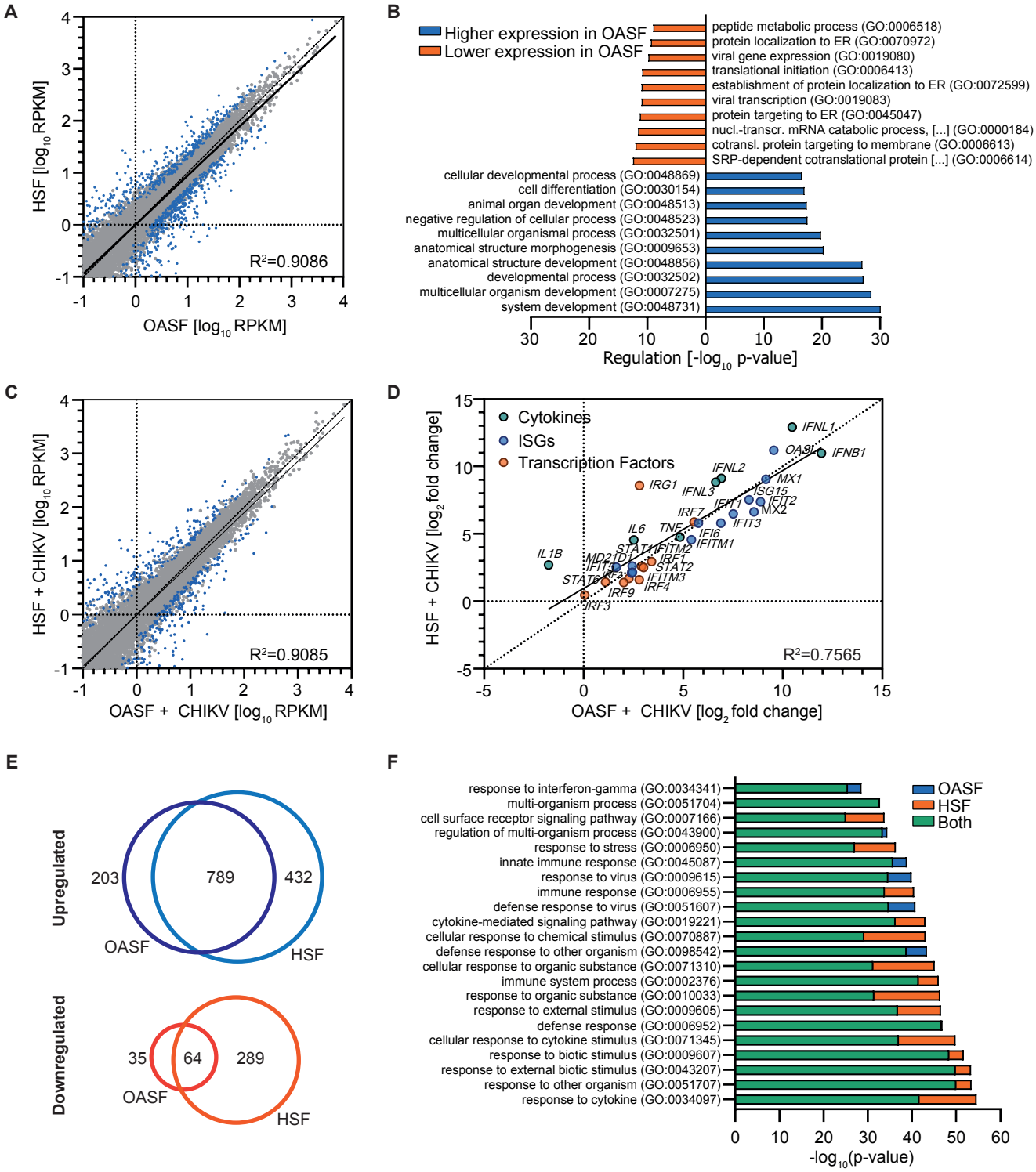
A
HSF [log10 RPKM]
OASF [log10 RPKM]
R²=0.9086
B
Higher expression in OASF
Lower expression in OASF
peptide metabolic process (GO:0006518)
protein localization to ER (GO:0070972)
viral gene expression (GO:0019080)
translational initiation (GO:0006413)
establishment of protein localization to ER (GO:0072599)
viral transcription (GO:0019083)
protein targeting to ER (GO:0045047)
nucl.-transcr. mRNA catabolic process, [...] (GO:0000184)
cotransl. protein targeting to membrane (GO:0006613)
SRP-dependent cotranslational protein [...] (GO:0006614)
cellular developmental process (GO:0048869)
cell differentiation (GO:0030154)
animal organ development (GO:0048513)
negative regulation of cellular process (GO:0048523)
multicellular organismal process (GO:0032501)
anatomical structure morphogenesis (GO:0009653)
anatomical structure development (GO:0048856)
developmental process (GO:0032502)
multicellular organism development (GO:0007275)
system development (GO:0048731)
Regulation [-log10 p-value]
C
HSF + CHIKV [log10 RPKM]
OASF + CHIKV [log10 RPKM]
R²=0.9085
D
Cytokines
ISGs
Transcription Factors
IFNL1
OAS1
IFNB1
IFNL2
MX1
IRG1
IFNL3
ISG15
IFIT2
IFIT1
MX2
IRF7
IFIT3
IL6
TNF
IFI6
IFITM1
STAT1
IFITM2
IL1B
MD21D1
IRF1
IFIT5
STAT2
STAT6
IFITM3
IRF4
IRF9
IRF3
HSF + CHIKV [log2 fold change]
OASF + CHIKV [log2 fold change]
R²=0.7565
E
Upregulated
203
789
432
OASF
HSF
Downregulated
35
64
289
OASF
HSF
F
OASF
HSF
Both
response to interferon-gamma (GO:0034341)
multi-organism process (GO:0051704)
cell surface receptor signaling pathway (GO:0007166)
regulation of multi-organism process (GO:0043900)
response to stress (GO:0006950)
innate immune response (GO:0045087)
response to virus (GO:0009615)
immune response (GO:0006955)
defense response to virus (GO:0051607)
cytokine-mediated signaling pathway (GO:0019221)
cellular response to chemical stimulus (GO:0070887)
defense response to other organism (GO:0098542)
cellular response to organic substance (GO:0071310)
immune system process (GO:0002376)
response to organic substance (GO:0010033)
response to external stimulus (GO:0009605)
defense response (GO:0006952)
cellular response to cytokine stimulus (GO:0071345)
response to biotic stimulus (GO:0009607)
response to external biotic stimulus (GO:0043207)
response to other organism (GO:0051707)
response to cytokine (GO:0034097)
-log10(p-value)

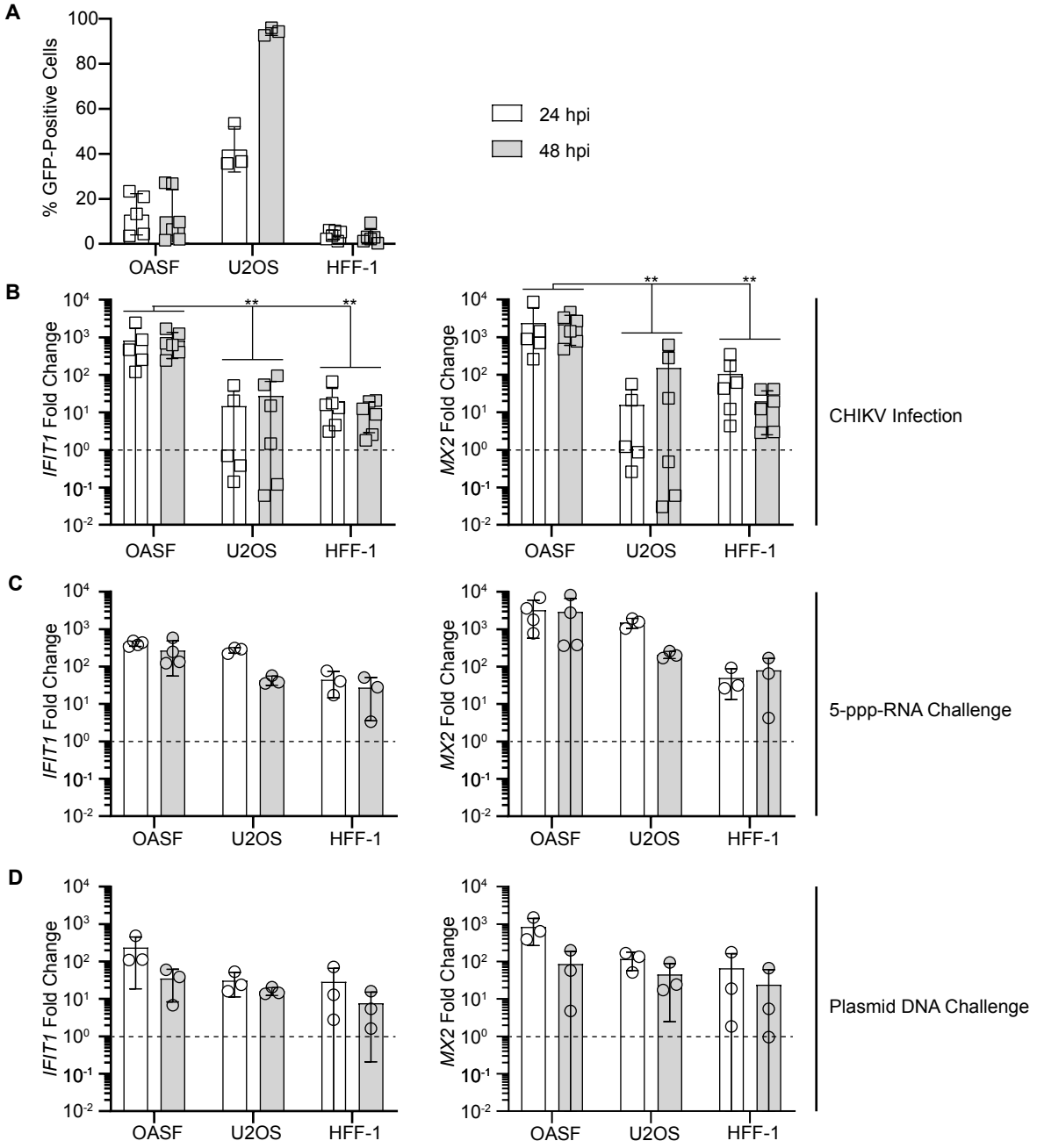
A
% GFP-Positive Cells
100
80
60
40
20
0
OASF
U2OS
HFF-1
24 hpi
48 hpi
B
IFIT1 Fold Change
MX2 Fold Change
**
**
CHIKV Infection
C
5-ppp-RNA Challenge
D
Plasmid DNA Challenge

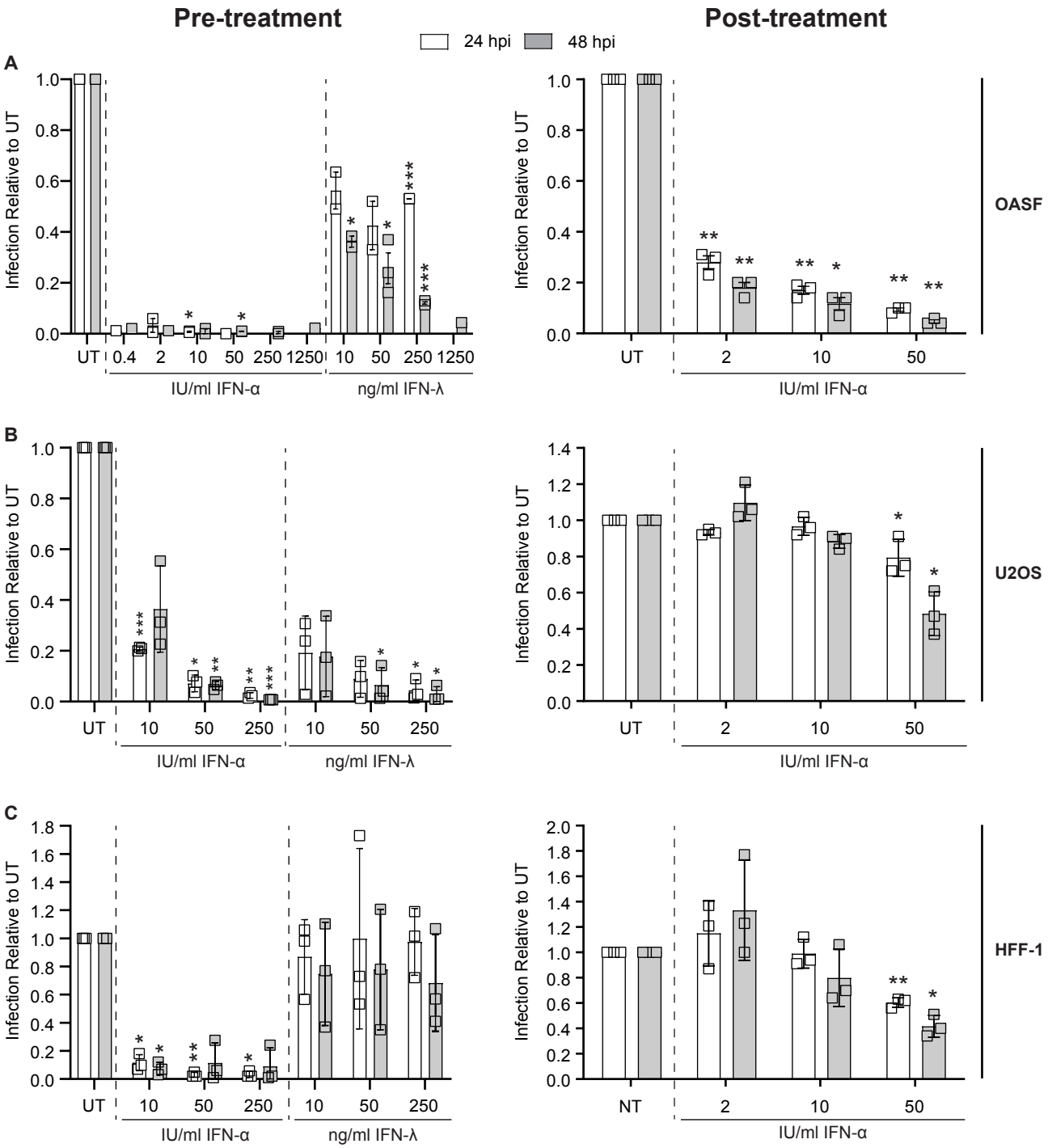
Pre-treatment
Post-treatment
24 hpi
48 hpi
A
B
C
Infection Relative to UT
UT
0.4
2
10
50
250
1250
IU/ml IFN-α
ng/ml IFN-λ
NT
OASF
U2OS
HFF-1